Progress In Electromagnetics Research Letters, Vol. 72, 75–81, 2018

Electrically-Small Circularly-Polarized Quasi-Yagi Antenna

Son Xuat Ta[1, 2, *]

Abstract—In this letter, an electrically-small circularly polarized (CP) quasi-Yagi antenna is presented. It is composed of three elements; i.e., a compact single-feed crossed-dipole antenna acted as the driver and two parasitic elements acted as the reflector and director, respectively. Each arm of all elements contains a meander line with an arrowhead ending to realize compactness. The driver has double vacant-quarter printed rings incorporated into it to generate the CP radiation. The parasitic elements are incorporated with the crossed-dipole driver to not only produce a directive radiation, but also broaden the antenna bandwidth. The final design with overall size of 35 mm × 35 mm × 27 mm ($0.184\lambda_o \times 0.184\lambda_o \times 0.142\lambda_o$ at 1.575 GHz, $ka = 0.93$) a measured 10-dB bandwidth of 19.23% (1.476–1.790 GHz), 3-dB axial ratio bandwidth of 7.67% (1.505–1.625 GHz), a broadside gain of 3.0 ± 0.2 dBic, and the maximum front-to-back ratio of 8.2 dB. The proposed antenna is applicable to a variety of wireless system operating near 1.575 GHz, such as Global Positioning Systems, Global Navigation Satellite Systems, as well as international maritime satellite organization (Inmarsat) networks.

1. INTRODUCTION

For many decades, electrically small antenna (ESA) is a hot topic in antenna research due to its compact form and potential usefulness in many wireless communication systems [1]. An antenna is considered as an ESA if it can be completely enclosed within a radian sphere [2]. A general characteristic of ESAs is that they operate in the fundamental dipole mode because of the ESAs possess small physical sizes in term of their operational wavelengths [3]. Therefore, a challenge in designing ESA is to achieve a directional radiation pattern. In order to address this issue, several ways of developing directive ESAs have been proposed. These ways, for instance, include: using electrically small reflectors [3–5] or directors [6], associating with ground plane [7, 8], arranging ESA elements in linear array [9], and constructing Huygens source antennas [10–12]. On the other hand, it well known that circularly polarized (CP) radiation has been used to combat multi-path interferences or fading, mitigate polarization mismatch losses, and reduce Faraday rotation effects caused by the ionosphere. Accordingly, several directive ESAs with CP radiation [4, 6–8, 10, 11] have been conducted. However, the main drawback of these CP ESAs is narrow axial ratio (AR) bandwidth, i.e., their 3-dB AR bandwidths are approximately 1% or less. In order to achieve a directive radiation, the near-field resonant parasitic (NFRP) element was designed to act a reflector of the crossed dipole antenna [13]. The NFRP reflector just strongly affects the directive pattern in the low-frequency region, and therefore, the unidirectional radiation is not very good in the high-frequency region.

This letter presents a CP ESA based on quasi-Yagi antenna configuration. The antenna consists of three elements, including a driver and two parasitic elements acted as the reflector and the director, respectively. The driver is a single-feed crossed-dipole, which is incorporated with double vacant-quarter printed rings to generate the CP radiation. Both reflector and director are shaped in orthogonal dipoles.

Received 24 October 2017, Accepted 21 November 2017, Scheduled 11 January 2018

* Corresponding author: Son Xuat Ta (tasonxuat@tdt.edu.vn).

[1] Division of Computational Physics, Institute for Computational Science, Ton Duc Thang University, Ho Chi Minh City 700000, Vietnam. [2] Faculty of Electrical and Electronics Engineering, Ton Duc Thang University, Ho Chi Minh City 700000, Vietnam.

To achieve the electrically-small form, a technique of using meander line with an arrowhead ending is applied for each arm of the three elements. The parasitic elements are designed to not only achieve a directional radiation pattern, but also enhance the operational bandwidth of the antenna. The antenna was first computationally characterized using the ANSYS/ANSOFT high frequency structure simulator (HFSS) and then validated experimentally.

2. ANTENNA DESIGN AND CHARACTERISTICS

2.1. Antenna Geometry

The antenna geometry is illustrated in Fig. 1, which is composed of three elements; a single-feed crossed-dipole acted as a driver and two parasitic elements acted as a reflector and a director, respectively. The reflector was printed on the bottom-side of substrate 1. The crossed-dipole driver was built on both sides of substrate 2. The director was printed on the top-side of substrate 3. All substrates are Rogers RT/Duroid^{TM} 5880 ($\varepsilon_r = 2.2$, $\tan\delta = 0.009$, and $h_{s1} = h_{s2} = 0.508\,\text{mm}$). For supporting the structure, two foam ($\varepsilon_r = 1.07$, $\mu_r = 1$, $\tan\delta = 0.0006$, and $H_1 = H_2 = 12.7\,\text{mm}$) were sandwiched between the three substrates. Each arm of the three elements contains a meander line with an arrowhead ending. The driver consists of double vacant-quarter printed rings. A coaxial line passed through the substrate 2 to feed the crossed-dipole driver directly. The antenna was optimized with a series of HFSS simulations to achieve a directive radiation and broadband characteristic near 1.575 GHz. Referring to Fig. 1, the optimized design parameters were: $h_{s1} = h_{s2} = h_{s3} = 0.508$, $H_1 = H_2 = 12.7$, $W_{ref} = 35$, $W_{b1} = 3.0$, $W_{c1} = 15.8$, $L_{b1} = 10$, $w_{i1} = 0.2$, $g_{i1} = 0.6$, $L_{i1} = 7$, $R_i = 3.7$, $W_r = 0.4$, $r_o = 1.5$, $w_{s1} = 2.0$, $W_{driv} = 35$, $W_{b2} = 3$, $W_{c2} = 18.5$, $L_{b2} = 10$, $w_{i2} = 0.2$, $g_{i2} = 0.6$, $L_{i2} = 7$, $w_{s2} = 1.4$, $W_{dir} = 35$, $W_{b3} = 3$, $L_{b3} = 10$, $w_{i3} = 0.2$, $g_{i3} = 0.6$, $L_{i3} = 7$ (units in mm).

2.2. Different Numbers of Element

For better understanding the radiation mechanism of the proposed antenna, we compared performances of the antenna for different numbers of elements. Fig. 2 shows the cross-sectional view of the antenna with different numbers of elements; the 1-element design is a single-feed crossed-dipole antenna. The 2-element design is the first one loaded with a parasitic element, which was acted as the reflector. The 3-element design is the proposed antenna including a single-feed crossed-dipole driver and two parasitic elements acted as the reflector and director, respectively. All configurations were designed with the same size of the substrate and optimized to achieve good impedance matching and AR characteristics near 1.6 GHz. Referring to Fig. 1(c), the design parameters of the 1-element antenna and are as follows: $h_{s2} = 0.508$, $W_{driv} = 35$, $W_{b2} = 3.2$, $W_{c2} = 17.5$, $L_{b2} = 10$, $w_{i1} = 0.2$, $g_{i1} = 0.6$, $L_{i1} = 7.0$, $R_i = 3.2$, $W_r = 0.5$, $r_o = 2.2$, $w_{s2} = 2.0$ (units in mm). The design parameters of the 2-element and 3-element designs are same as those of the proposed antenna in Fig. 1. The three designs were characterized via the HFSS, and their results are given in Figs. 3 and 4.

Figure 3 shows the simulated $|S_{11}|$ and AR values of the three designs. The 1-element antenna yielded a $|S_{11}| < -10\,\text{dB}$ bandwidth of 1.565–1.790 GHz (13.4%) with two resonances at 1.60 GHz and 1.72 GHz and a 3-dB AR bandwidth of 1.60–1.64 GHz (2.4%) with one minimum AR point at 1.62 GHz (AR = 1.84 dB). Due to the presence of the parasitic elements, the impedance matching and 3-dB AR bandwidths were broadened significantly. The 2-element antenna yielded a $|S_{11}| < -10\,\text{dB}$ bandwidth of 1.465–1.760 GHz (18.3%) with multiple resonances and a 3-dB AR bandwidth of 1.50–1.625 GHz (8.0%) with two minimum AR points at 1.515 GHz (AR = 1.9 dB) and 1.58 GHz (AR = 0.42 dB). The proposed design yielded a $|S_{11}| < -10\,\text{dB}$ bandwidth of 1.477–1.748 GHz (16.8%) and a 3-dB AR bandwidth of 1.508–1.628 GHz (7.7%) with two minimum AR points at 1.523 GHz (AR = 0.76 dB) and 1.596 GHz (AR = 1.72 dB). This bandwidth-enhanced phenomenon was presented and discussed in [13]; i.e., the parasitic elements are designed to work as near-field resonant parasitic elements, which produce the extra resonances and CP radiations for the antenna system. These extra ones are combined with the resonances and CP radiations caused by the driver to broaden the antenna bandwidth.

In the proposed 3-element design, the director was not designed to broaden the bandwidth, which was used to improve the radiation characteristics of the antenna. Fig. 4 shows the simulated broadside gains and front-to-back (F-B) ratios, including 1.6-GHz 3D radiation patterns, of the three designs.

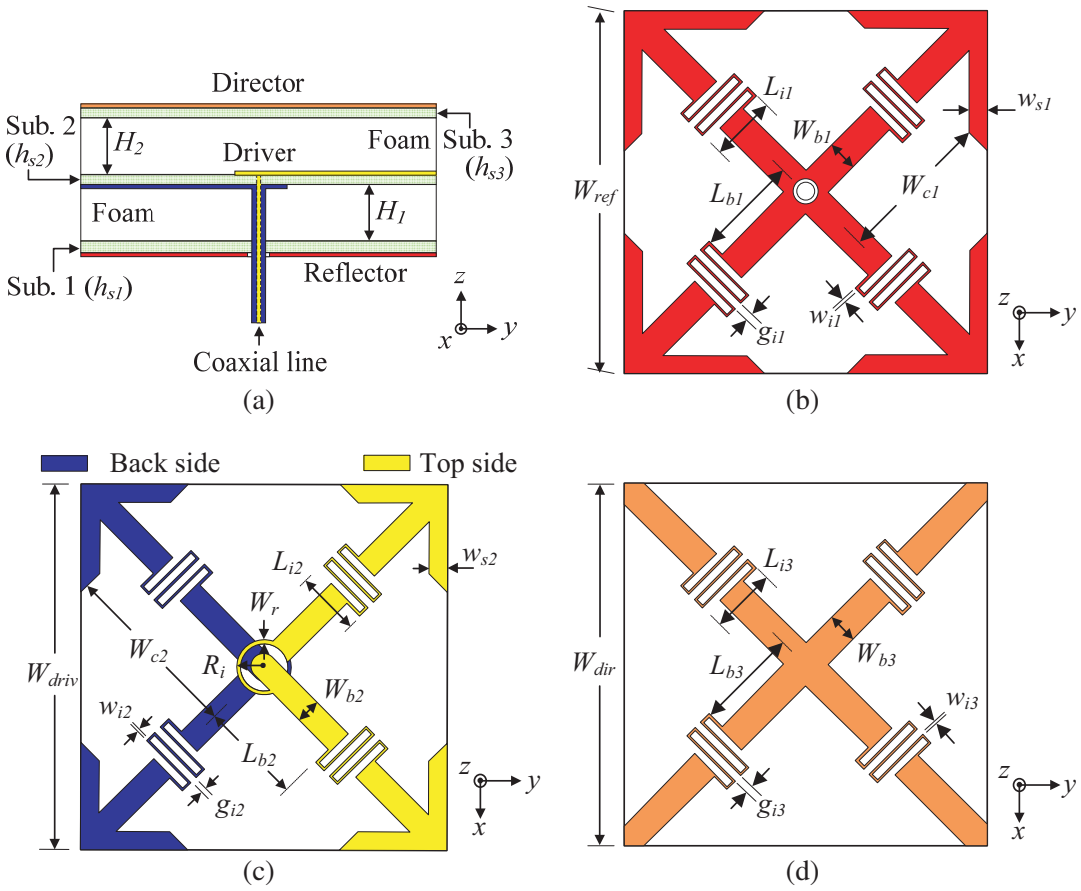

Figure 1. Geometry of the antenna: (a) cross-sectional-view, (b) top-view of reflector, (c) top-view of crossed-dipole driver, and (d) top-view of director.

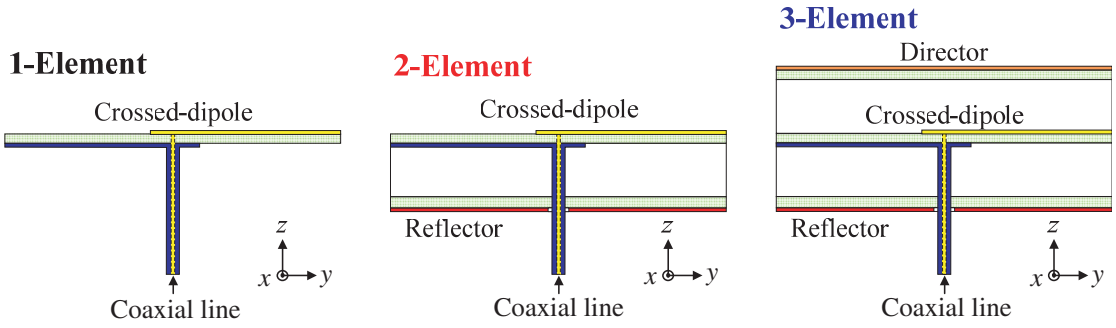

Figure 2. Cross-sectional view of the antenna with different numbers of element.

The 1-element antenna radiates equally well in the broadside and backside ($\pm z$) directions within the examined frequency range. At 1.60 GHz, the compact crossed-dipole without parasitic element yielded a bidirectional radiation pattern with a gain of approximately 1.2 dBic in both the $\pm z$ directions. Due to the presence of the reflector, the broadside gain increased, whereas the backside radiation decreased. The 2-element design yielded broadside gain of 2.45 ± 0.3 dBic and a backside gain ranging from -4.1 dBic to 0.12 dBic within its 3-dB AR bandwidth. However, the broadside radiation of the 2-element antenna was not very good in the high-frequency region because of the reflector element strongly affected the radiation characteristics in the low-frequency region only. At 1.6 GHz, the 2-element antenna had a 2.59 dBic gain in the broadside direction and a -0.17 dBic gain in the backside direction, resulting in

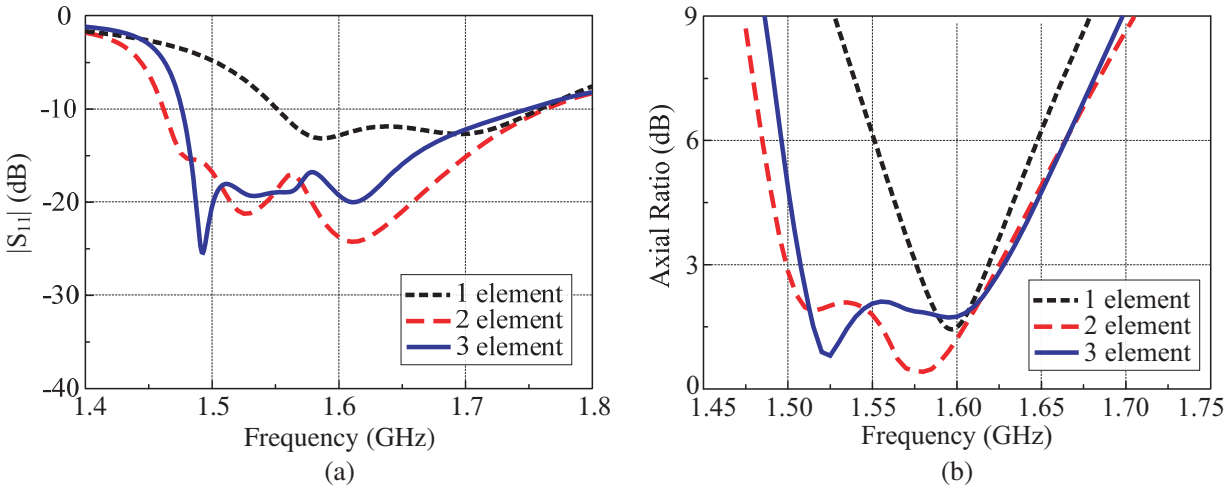

Figure 3. Simulated (a) $|S_{11}|$ and AR values of the antenna for different numbers of element.

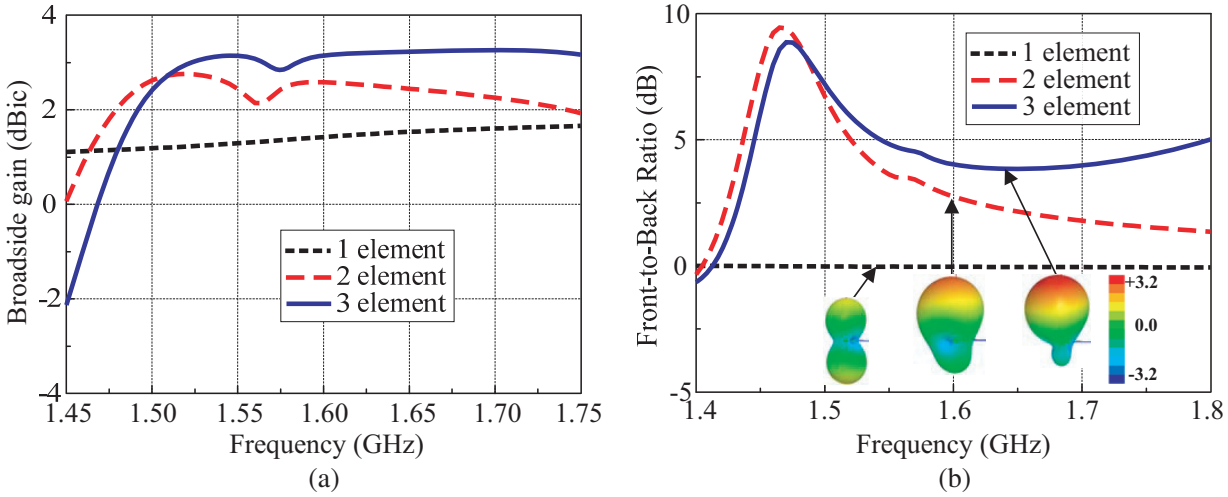

Figure 4. Simulated (a) broadside-gain and (b) front-to-back ratio and 1.6-GHz 3D radiation pattern of the antenna for different numbers of element.

an F-B ratio of 2.76 dB. In order to improve the broadside radiation in the high-frequency region, i.e., increasing broadside gain and reducing the backside radiation, we added more one parasitic element acted as the director. The 3-element design yielded higher gain and F-B ratio as compared to the other designs; its broadside gain was 3.1 ± 0.1 dBic and its F-B ratio was > 3.85 dB within the 3-dB AR bandwidth. At 1.6 GHz, the proposed antenna had a 3.15 dBic gain in the broadside direction and -0.9 dBic gain in the backside direction, resulting in an F-B ratio of 4.05 dB. Furthermore, the HFSS simulations indicate that the broadside radiation of the antenna can be improved by adding more director elements. However, this improvement is accompanied with increasing the electrical size of the antenna. For an electrically small size ($ka < 1$), the 3-element design is chosen for the final design.

3. MEASUREMENTS

For verification, the 3-element antenna was fabricated and measured. Its elements were realized on the Rogers RT/DuroidTM 5880 substrates with 17-µm copper thickness via a standard wet-etching technology. A sample of the fabricated prototype is shown in Fig. 5. For a simply fabrication, the substrates and supporting foams were fastened together using thin strips of tape (not included in the

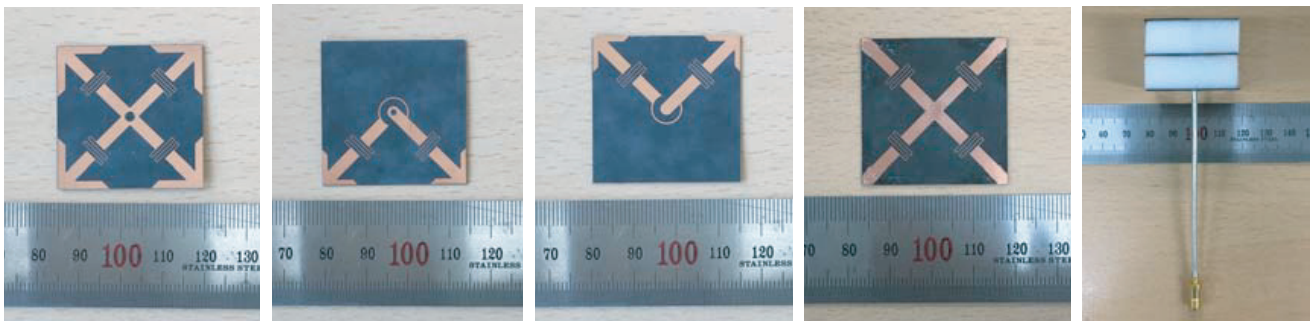

(a) (b) (c) (d) (e)

Figure 5. Fabricated sample of the antenna; (a) the reflector; (b) back-side of the driver; (c) top-side of the driver; (d) the director; and (e) side-view including the coaxial line.

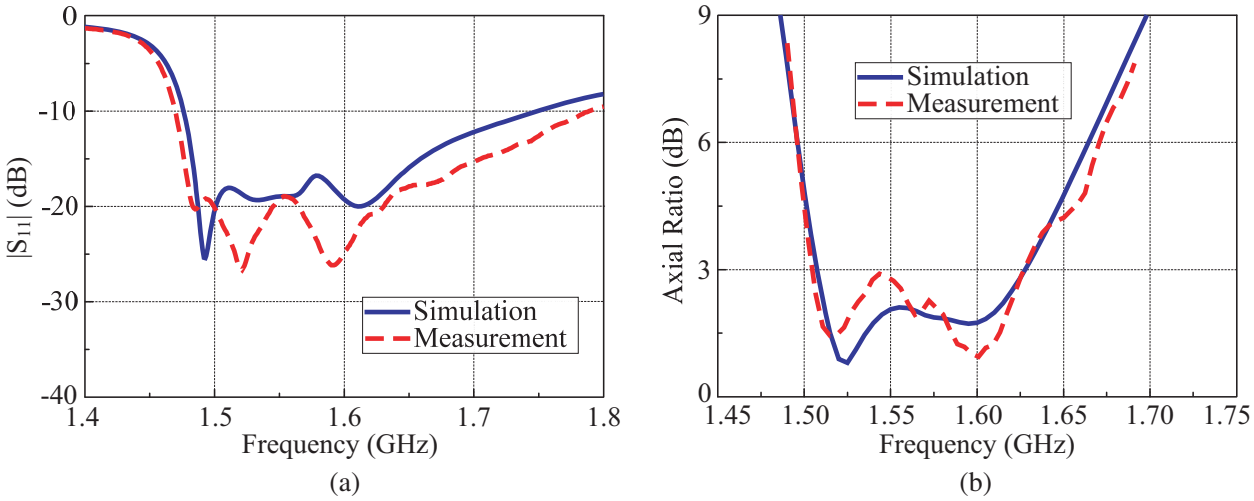

Figure 6. Measurement and simulation results of the proposed antenna: (a) $|S_{11}|$ and (b) AR values.

simulations). It has an overall size of 35 mm × 35 mm × 27 mm ($0.184\lambda_o \times 0.184\lambda_o \times 0.142\lambda_o$ at 1.575 GHz) and an electrically small size ($ka = 0.93$ at 1.575 GHz).

Figure 6 shows the comparison between the measured and simulated $|S_{11}|$ and AR values for the prototype. It is observed that the measurements agreed rather closely with the HFSS simulations. As shown in Fig. 6(a), the measurements resulted in a $|S_{11}| < -10$ dB bandwidth of 19.23% (1.476–1.790 GHz), while the HFSS predicted value was 16.8% (1.477–1.748 GHz). As shown in Fig. 6(b), the measurements resulted in an AR < 3.0 dB bandwidth of 7.67% (1.505–1.625 GHz) in contrast to the simulated value of 7.7% (1.508–1.628 GHz).

Figure 7 shows the normalized gain patterns of the proposed antenna at 1.525 GHz and 1.60 GHz. Both the simulations and measurements show that the antenna generates good broadside RHCP radiation with a highly symmetric profile in both the x-z and y-z planes. At 1.525 GHz, the measurements yielded an F-B ratio of 4.5 dB and half-power beamwidths (HPBWs) of 115° and 109° in the x-z and y-z planes, respectively. At 1.60 GHz, the measurements yielded an F-B ratio of 3.5 dB and HPBWs of 118° and 111° in the x-z and y-z planes, respectively. There were some ripples in the measured results, which could be attributed to the effects of the foam rack and the thin tapes used in the pattern measurement setup.

Figure 8 illustrates the simulated and measured broadside gains and F-B ratios of the fabricated prototype. As shown in Fig. 8(a), within the CP radiation bandwidth, the measurements resulted in a broadside gain of 3.0 ± 0.2 dBic, while the HFSS simulations predicted a broadside gain of 3.1 ± 0.1 dBic. As shown in Fig. 8(b), the measurements yielded an F-B ratio of > 3.2 dB with the maximum value

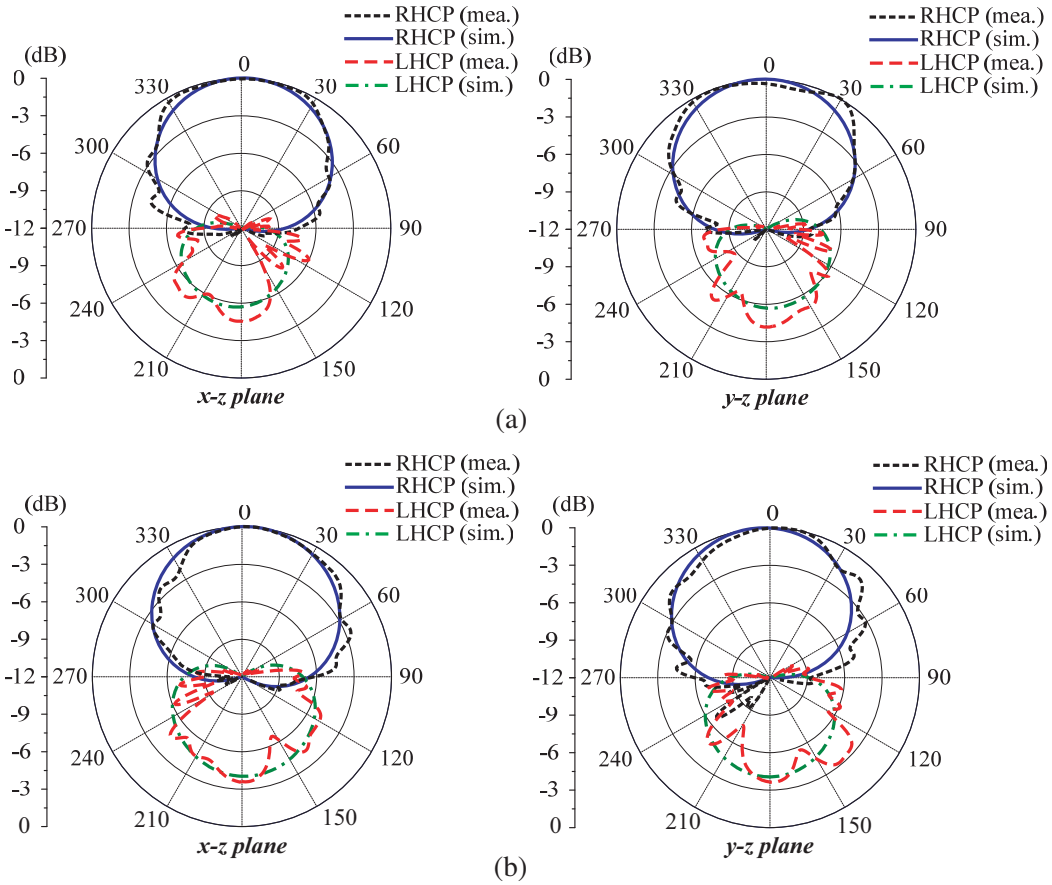

Figure 7. Normalized gain-patterns of the proposed antenna at (a) 1.525 GHz and (b) 1.60 GHz.

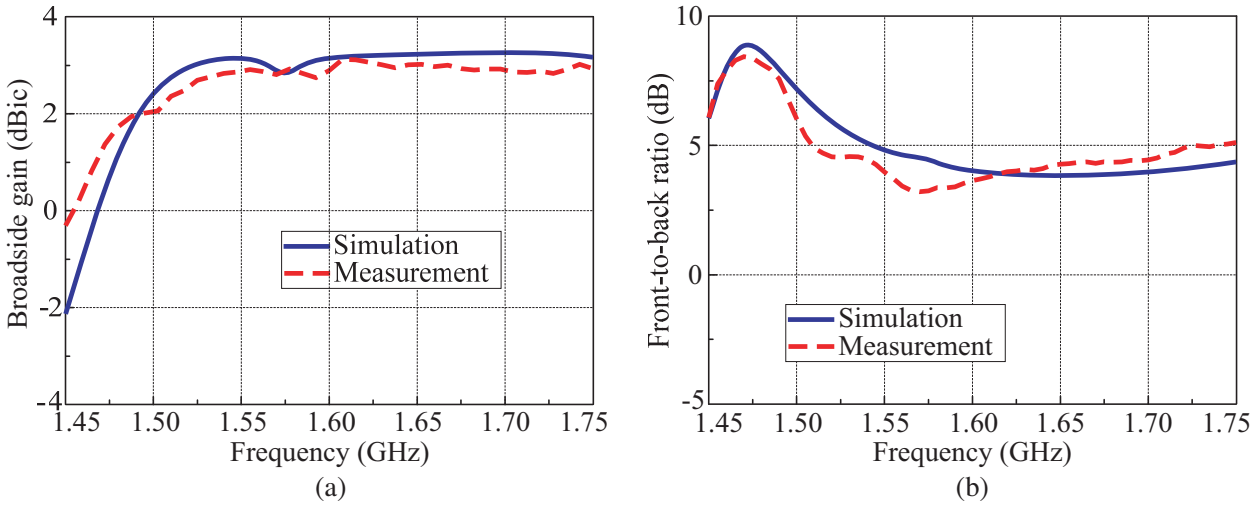

Figure 8. Measurement and simulation results of the proposed antenna: (a) broadside gain and (b) front-to-back ratio.

of 8.2 dB at 1.470 GHz, whereas the HFSS simulations resulted in an F-B ratio of > 3.85 dB and the maximum value of 8.9 dB at 1.472 GHz. Additionally, the measurements found an average RE of 75%, as compared to the simulated value of 78%, across the 3-dB AR bandwidth.

4. CONCLUSION

A three-element CP quasi-Yagi antenna with electrically-small size has been presented. The antenna consists of a compact single-feed crossed-dipole driver and two parasitic elements, which act as reflector and director. The parasitic elements are employed for not only obtaining a directive radiation, but also broadening the antenna bandwidth in terms of impedance matching and CP radiation. The final design with overall size of $35\,\text{mm} \times 35\,\text{mm} \times 27\,\text{mm}$ ($0.184\lambda_o \times 0.184\lambda_o \times 0.142\lambda_o$ at 1.575 GHz) has been fabricated and measured. It has a measured $|S_{11}| < -10\,\text{dB}$ bandwidth of 19.23% (1.476–1.790 GHz), 3-dB axial ratio bandwidth of 7.67% (1.505–1.625 GHz), broadside gain of $3.0 \pm 0.2\,\text{dBic}$, maximum F-B ratio of 8.2 dB, and average efficiency of 75%. With the advantages of electrically-small size, broadband, directive radiation pattern, and high RE, the antenna can be widely used in a variety of wireless systems operating near 1.575 GHz, such as Global Positioning Systems, Global Navigation Satellite Systems, as well as international maritime satellite organization (Inmarsat) networks.

REFERENCES

1. Sievenpiper, D. F., D. C. Dawson, M. M. Jacob, T. Kanar, S. Kim, J. Long, and R. G. Quarfoth, "Experimental validation of performance limits and design guidelines for small antennas," *IEEE Trans. Antennas Propag.*, Vol. 60, No. 1, 8–19, Jan. 2012.
2. Hansen, R., "Fundamental limitations in antennas," *Proc. IEEE*, Vol. 69, No. 2, 170–182, Feb. 1981.
3. Tang, M., R. W. Ziolkowski, S. Xiao, and M. Li, "A high-directivity, wideband, efficient, electrically small antenna system," *IEEE Trans. Antennas Propag.*, Vol. 62, No. 12, 6541–6547, Dec. 2014.
4. Jin, P. and R. W. Ziolkowski, "High directivity, electrically small, low-profile, near-field resonant parasitic antennas," *IEEE Antennas Wireless Propag. Lett.*, Vol. 11, 305–309, 2012.
5. Tang, M. and R. W. Ziolkowski, "A study of low-profile, broadside radiation, efficient, electrically small antennas based on complementary split ring resonators," *IEEE Trans. Antennas Propag.*, Vol. 61, No. 9, 4419–4430, Sep. 2013.
6. Yu, J. and S. Lim, "Design of an electrically small, circularly polarized, parasitic array antenna for an 433.92-MHz RFID handheld reader," *IEEE Trans. Antennas Propag.*, Vol. 60, No. 5, 2549–2554, May 2012.
7. Jin, P. and R. W. Ziolkowski, "Multi-frequency, linear and circular polarized, metamaterial-inspired, near-field resonant parasitic antennas," *IEEE Trans. Antennas Propag.*, Vol. 59, No. 5, 1446–1459, May 2011.
8. Sun, L., B. Du, and B. Sun, "Inductively loaded and magnetically coupled small antenna with circular polarization," *Journal of Electromagnetic Waves and Applications*, Vol. 27, No. 5, 539–543, 2013.
9. Haskou, A., A. Sharaiha, and S. Collardey, "Design of small parasitic loaded superdirective end-fire antenna arrays," *IEEE Trans. Antennas Propag.*, Vol. 63, No. 12, 5456–5464, Dec. 2015.
10. Alitalo, P., A. O. Karilainen, T. Niemi, C. R. Simovski, and S. A. Tretyakov, "Design and realisation of an electrically small Huygens source for circular polarisation," *IET Microw. Antennas Propag.*, Vol. 5, No. 7, 783–789, 2011.
11. Morlaas, C., B. Souny, and A. Chabory, "Helical-ring antenna for hemispherical radiation in circular polarization," *IEEE Trans. Antennas Propag.*, Vol. 63, No. 11, 4693–4701, Nov. 2015.
12. Tang, M., H. Wang, and R. W. Ziolkowski, "Designing and testing of simple, electrically small, low-profile, Huygens source antennas with broadside radiation performance, *IEEE Trans. Antennas Propag.*, Vol. 64, No. 11, 4607–4617, Nov. 2016.
13. Ta, S. X., I. Park, and R. W. Ziolkowski, "Compact crossed-dipole antenna loaded with near-field resonant parasitic element," *IEEE Access*, Vol. 5, 14657–14663, 2017.